Bimetallic Nanocrystals

DOI: 10.1002/anie.201206044

Synthesis of Pd-Rh Core–Frame Concave Nanocubes and Their Conversion to Rh Cubic Nanoframes by Selective Etching of the Pd Cores**

*Shuifen Xie, Ning Lu, Zhaoxiong Xie, Jinguo Wang, Moon J. Kim, and Younan Xia**

Controlling the shape, morphology, and/or structure of nanocrystals has been a subject of intensive research because it allows the properties of nanocrystals to be tailored, thus enhancing their applications in catalysis, electronics, photonics, sensing, and biomedical research.[1–5] For noble metals, they tend to form polyhedrons with a solid structure and enclosed by a convex surface consisting of low-index facets, such as {111}, {100}, and {110} in different proportions. Therefore, the most commonly observed shapes are octahedrons, cuboctahedrons, and cubes, with different degrees of truncation at corners and edges. Herein we report a facile synthesis of Pd-Rh bimetallic nanocubes with a novel core–frame structure and concave side faces by combining kinetic control with surface capping, and their subsequent conversion to Rh cubic nanoframes by selective removal of the Pd cores by wet etching.

Nanocrystals with hollow structures and/or concave faces have recently started to receive great interest owing to the presence of high-index facets on their surfaces, as well as unique optical and catalytic properties. Notable examples include nanocubes with concave side faces, nanocages (hollow cubes with pores in the walls), and nanoframes (hollow cubes only with ridges and no side faces).[2–4] Such nanocrystals have been reported for a number of metals, including Au, Ag, Pd, Pt, and Rh,[3–5] although most of them were made of a single metal. There are only a few reports on bimetallic systems, including core–shell concave nanocrystals in the composition of Pt@Rh, Au@Pd, and Pd@Au.[5e,6,7] Owing to the formation of a core–shell structure, only those atoms situated on the outer surface of such a bimetallic nanocrystal are available for catalyzing chemical reactions. In comparison, it will be a significant advantage to formulate a bimetallic nanocrystal into a core–frame structure, in which the atoms of both the core and frame portions will be accessible to reactants.

Seed-mediated growth has been widely used by many groups for generating bimetallic nanocrystals,[6–8] but most of the products are limited to the core–shell structure. It remains a major challenge to achieve site-selective deposition of the second metal on the seed and thus generate an incomplete shell. Most recently, our group demonstrated that kinetic control is a simple and versatile means for achieving site-selective overgrowth.[7,9] By controlling the rate at which Ag atoms are formed in a solution, for example, we could confine the nucleation and growth of Ag to one, three, or six of the {100} side faces of a Pd cubic seed.[9] As a result, Pd-Ag bimetallic nanocrystals with both Pd and Ag being exposed on the surface were obtained in high yields. Herein we demonstrate another type of site-specific growth in which Rh atoms are only allowed to nucleate and grow at the corners and edges of Pd cubic seeds to generate Pd-Rh nanocubes with a core–frame structure and concave side faces. The spatial confinement was achieved through a combination of kinetic control and selective capping of Pd {100} facets by Br^- ions. As Rh is highly resistant to oxidative corrosion,[10] the Pd-Rh core–frame nanocubes were subsequently converted into Rh cubic nanoframes with a highly open structure by selective etching of the Pd cores.

Figure 1 shows a summary of all the major steps involved in the formation of Pd-Rh bimetallic nanocubes with a core–frame structure and concave side faces, and their subsequent conversion into Rh cubic nanoframes. Firstly, uniform Pd nanocubes of 18 nm in edge length (Supporting Information, Figure S1) were prepared by reducing Na_2PdCl_4 with L-ascorbic acid (AA) in an aqueous solution with Br^- ions serving as a capping agent for the Pd(100) surface.[11] The as-obtained Pd nanocubes were slightly truncated at all corners and edges, with the surface being mainly covered by the Br^--capped {100} facets. These Pd cubes were then used as seeds for the overgrowth of Rh atoms in the presence of Br^- ions.

[*] S. Xie, Prof. Y. Xia
The Wallace H. Coulter Department of Biomedical Engineering, Georgia Institute of Technology and Emory University, School of Chemistry and Biochemistry and School of Chemical and Biomolecular Engineering, Georgia Institute of Technology
Atlanta, GA 30332 (USA)
E-mail: younan.xia@bme.gatech.edu

S. Xie, Prof. Z. Xie
State Key Laboratory for Physical Chemistry of Solid Surfaces and Department of Chemistry College of Chemistry and Chemical Engineering, Xiamen University
Xiamen 361005 (P. R. China)

Dr. N. Lu, Dr. J. Wang, Prof. M. J. Kim
Department of Materials Science and Engineering, University of Texas at Dallas
Richardson, TX 75080 (USA)

Prof. M. J. Kim
Department of Nanobio Materials and Electronics, World Class University, Gwangju Institute of Science and Technology
Gwangju 500-712 (Korea)

[**] This work was supported in part by a grant from the NSF (DMR-1215034) and start-up funds from Georgia Institute of Technology. As a visiting student from Xiamen University, S.X. was also partially supported by the China Scholarship Council (CSC). N.L., J.W., and M.J.K. were supported by the World Class University Program from MEST through NRF (R31-10026).

Supporting information for this article is available on the WWW under http://dx.doi.org/10.1002/anie.201206044.

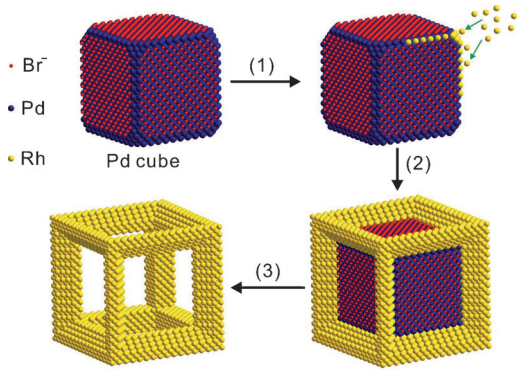

Figure 1. The three major steps involved in the synthesis of Pd-Rh core–frame nanocubes with concave faces and Rh cubic nanoframes. 1) Selective nucleation of Rh at the corners and edges of the Pd nanocubes owing to the capping of {100} side faces by Br^- ions; 2) formation of Pd-Rh bimetallic core–frame concave nanocubes as the growth of Rh on the corners and edges of the Pd nanocubes is continued; and 3) formation of Rh cubic nanoframes by selectively etching away the Pd cores.

The Rh precursor was introduced at a relatively slow rate using a syringe pump to avoid self-nucleation and to achieve kinetically controlled growth. The adsorbed Br^- ions prevented the newly formed Rh atoms from nucleating on the {100} side faces, so the Rh atoms could only nucleate at the corners and edges of a Pd cubic seed. With the deposition of Rh atoms at all corners and edges, we obtained Pd-Rh bimetallic nanocubes with a core–frame structure and concave faces, the surface of which was covered by Pd {100} and Rh {110} facets. In the last step, the Pd cubic cores were selectively dissolved from the Pd-Rh core–frame nanocubes using an aqueous etchant based on the Fe^{III}/Br^- pair, generating Rh cubic nanoframes with a unique open structure.

The synthesis of the Pd-Rh core–frame nanocubes was conducted in a solution of ethylene glycol (EG) containing poly(vinyl pyrrolidone) (PVP), AA, KBr, and the 18 nm Pd cubic seeds at 140 °C. The Na_3RhCl_6 solution (in EG) was introduced at a slow rate of 4.0 mL h^{-1} by the use of a syringe pump (see the Supporting Information for details). Our previous studies on the preparation of Rh concave nanocubes and multipods have shown that the reduction of Rh^{III} was extremely fast under the experimental conditions.[5e] As a result, the overall formation rate of Rh atoms was determined by the pumping rate, and the concentration of Rh atoms in the reaction system could thus be maintained at a very low level to achieve kinetically controlled growth. Under this condition, self-nucleation of Rh could be avoided, providing opportunities for the generated Rh atoms to nucleate and grow on the Pd seeds only. Figure 2 shows TEM images of the products obtained at different stages of a synthesis, clearly detailing the evolution from Pd nanocubes to Pd-Rh concave nanocubes with a core–frame structure. In the initial stage of the synthesis, the shape and size of the obtained Pd-Rh nanocrystals (Figure 2a) seemed to be almost identical to those of the initial Pd nanocubes when a relatively small amount (1.0 mL) of Na_3RhCl_6 was added. However, a close examination by high-resolution high-angle annular dark-field scanning transmission electron microscopy (HAADF-STEM) imaging (Figure 2b and c) clearly shows that the corners of the Pd nanocubes were slightly protruded. There are distinct atomic steps extending from the corner to the edge, suggesting that the overgrowth of Rh atoms started from the corners of a Pd seed and then extended to the edges. With the addition of more Na_3RhCl_6 solution, the resultant Rh atoms were continuously deposited onto the corners and edges. As shown by the TEM images in Figure 2d–f, the extent of concavity for the Pd-Rh core–frame nanocubes and the average edge length both increased as more Na_3RhCl_6 solution was added. After 6.0 mL of the Na_3RhCl_6 solution had been pumped into the reaction solution, the edge length of the final products reached about 24 nm. Because most of the Pd-Rh core–frame concave nanocubes were projecting along the $<100>$ direction on the copper gird, the corners appeared darker than the edges. This also explains why the out-extending corners gave the final products a pod-like appearance. When the synthesis was conducted in the absence of additional Br^- ions, the resultant Rh atoms also nucleated and grew on the side faces of a Pd seed in addition to the corners and edges (Supporting Information, Figure S2), demonstrating the blocking effect enabled by the Br^- ions adsorbed on the Pd(100) surface.

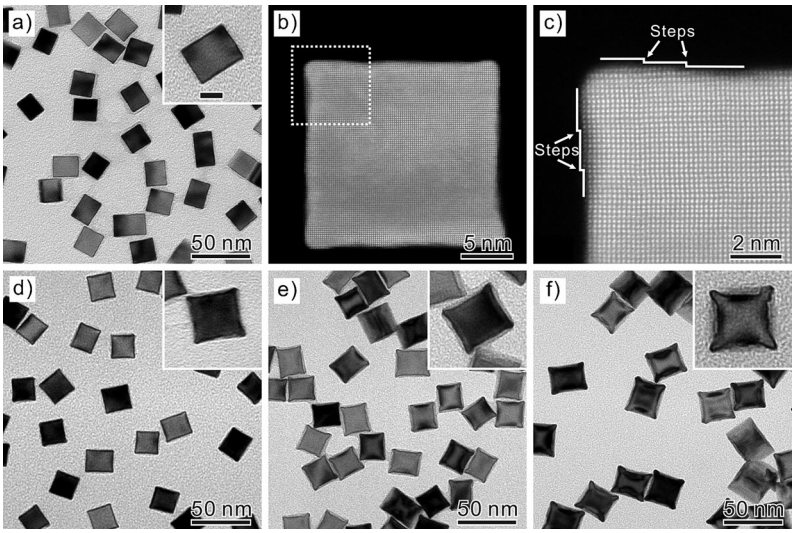

Figure 2. TEM images of Pd-Rh core–frame, concave nanocubes prepared using the standard procedure after different volumes of Na_3RhCl_6 solution in EG (2.5 mg mL^{-1}) had been added into the reacting system: a) 1.0, d) 2.0, e) 4.0, and f) 6.0 mL. b), c) High-resolution HAADF-STEM images of a single Pd-Rh nanocube shown in (a) and the region marked in (b). The scale bar in the first inset is 10 nm, and applies to all other insets.

The structure and composition of the bimetallic Pd-Rh nanocrystals in Figure 2f were further characterized by

scanning electron microscope (SEM), HAADF-STEM, and energy dispersive X-ray (EDX) analyses (both line scanning and mapping). As shown in Figure 3a and b, most of the Pd-Rh nanocrystals still had a cubic shape, together with a core–frame structure and concave faces. The side face of each Pd-Rh nanocube could be described as a "picture" in Pd encased by a "frame" made of Rh (see the inset in Figure 3a). From the high-resolution HAADF-STEM image (Figure 3c) of an individual Pd-Rh concave nanocube, which was projected along ⟨100⟩ zone axes, it can be clearly seen that, apart from the corners, Rh also grew on the edges of a Pd cubic seed to generate a perfect core–frame structure. A set of TEM images of Pd-Rh concave nanocubes were recorded (Supporting Information, Figure S3) from the same area of a copper grid at different tilting angles, further confirming the concave, core–frame structure. Figure 3d shows a HRTEM image, and the lattice fringe spacing of 1.35 and 1.92 Å marked on a corner and an edge of a concave nanocube can be indexed to the {220} and {200} reflections, respectively, of *fcc* Rh. Interestingly, the side surfaces of the out-extending edges were parallel to the {220} planes, forming an projection angle of 45° with the {100} planes. This result suggested that the out-extending Rh portion was dominated by Rh {110} facets. As the lattice mismatch between Pd and Rh is only 1.5%, it was impossible to differentiate the elemental compositions from lattice spacing. We applied EDX analyses to further determine the distributions of Pd and Rh in the core–frame concave nanocube. The EDX mapping (Figure 3e) clearly shows a color difference between the core (Pd, red) and the frame (Rh, green). Line scan profiles along corner-to-corner and edge-to-edge directions of a single Pd-Rh concave nanocube (Figure 3f and g) further confirm that the out-extending corners and edges were dominated by Rh, while the cubic core was essentially made of pure Pd.

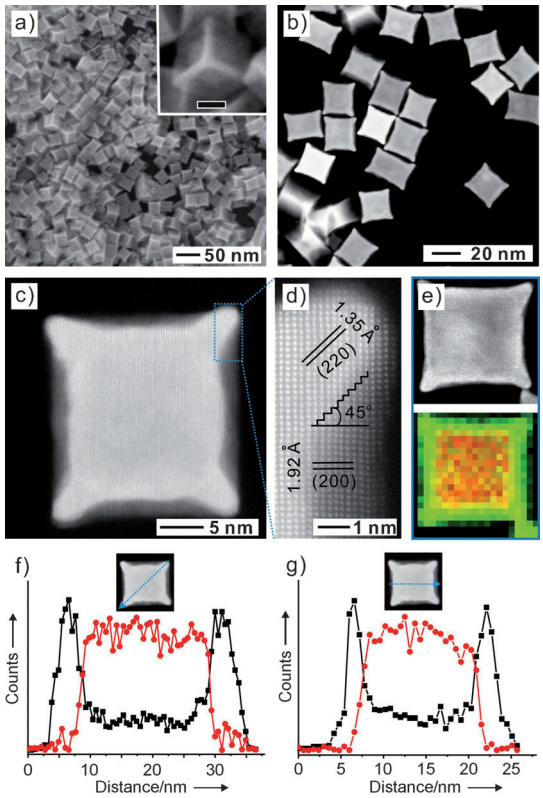

Figure 3. Structural and compositional characterizations of the Pd-Rh core–frame, concave nanocubes synthesized using the standard procedure: a) SEM images; b),c) HAADF-STEM images; d) high-resolution HAADF-STEM image of the region marked in (c); e) HAADF-STEM image together with the EDX mapping of an individual Pd-Rh nanocube (red = Pd, green = Rh); and f),g) line scan profiles recorded from a single Pd-Rh nanocube along the face diagonal and edge directions, respectively. Rh black ■, Pd red ●. The scale bar in the inset of (a) is 10 nm.

As demonstrated in previous studies, both Pd and Rh nanocrystals play important roles in the area of catalysis, such as Suzuki coupling, CO oxidation, and hydrogenation reactions.[12,13] Theoretically, for nanocrystals of *fcc* metals, the surface free energies of low-index facets increase in the order of $\gamma_{\{111\}} < \gamma_{\{100\}} < \gamma_{\{110\}}$. As the catalytic activities can be enhanced with the increase of surface energies, it should be expected that these bimetallic core–frame concave nanocubes with both Pd {100} and Rh {110} facets simultaneously exposed on the surface could provide some unique features for catalytic reactions. On the other hand, it is worth noting that there are differences in chemical stability and reactivity between Pd and Rh. Specifically, Rh is highly resistant to oxidative corrosion and can hardly be dissolved by aqua regia.[10] On the contrary, Pd is much more susceptible to chemical oxidation. Based on this difference in reactivity, we could selectively remove the Pd cubic cores from the Pd-Rh core–frame nanocubes to generate Rh nanoframes by chemical etching.

The etching was conducted in an aqueous solution at 100 °C by using an etchant based on the Fe^{III}/Br^{-} pair, with the addition of HCl to avoid the formation of insoluble $Fe(OH)_2$ (see the Supporting Information). As shown by the TEM image in Figure 4a, most of the Pd cubic cores were selectively removed, leaving behind Rh cubic nanoframes with a unique open structure. This result further confirms that the Pd-Rh concave nanocubes had a core–frame structure. Figure 4b and c shows TEM images of the Rh cubic nanoframes projected along ⟨100⟩ and ⟨110⟩ directions, respectively. The Rh ridges in the cubic nanoframe were only about 3 nm in thickness. Figure 4d shows a 3D atomic model of the nanoframe and its projections along different zone axes. Figure S4 shows a series of TEM images of Rh nanoframes that were recorded from the same area of a copper grid at different tilt angles, further confirming the open, frame-like structure. Figure S5 shows an EDX spectrum of the cubic nanoframes, indicating that they were consisted of pure Rh. When Pd-Rh core–frame nanocubes with less amounts of Rh deposited on the corners and edges were subjected to etching, the as-obtained Rh frames tended to be broken as the Rh ridges were too thin to provide enough mechanical strength (Supporting Information, Figure S6). The cubic nanoframes of Rh were thermally stabile up to 500 °C as the frame structure was well preserved after the sample had been heated at this temperature for 1 h (Supporting Information, Figure S7).

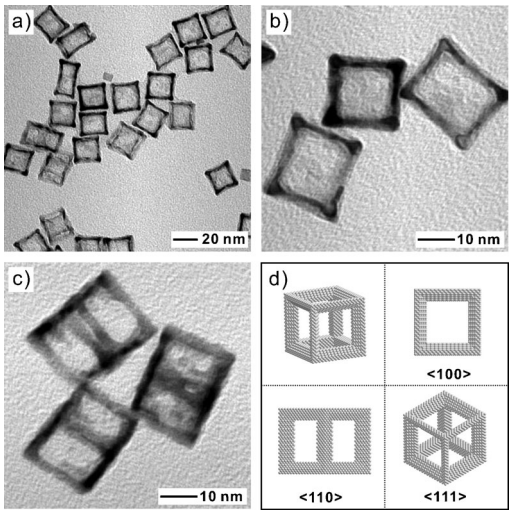

Figure 4. a) TEM images of Rh cubic nanoframes obtained by selectively etching away the Pd cores from the Pd-Rh core–frame nanocubes; b), c) TEM images of Rh cubic nanoframes projected along ⟨100⟩ and ⟨110⟩ zone axes, respectively; and d) drawings that present a 3D model of the Rh cubic nanoframe and its projections along ⟨100⟩, ⟨110⟩, and ⟨111⟩ zone axes.

The mechanism of etching can be understood from the standard electrical potentials of the redox species involved in this system. Owing to its relatively high reduction potential (Fe^{III}/Fe^{II}, 0.77 V vs. the standard hydrogen electrode or SHE), Fe^{III} is a well-known wet etchant for precious metals.[14] We have demonstrated that small multiple twinned particles of Pd could be selectively removed through oxidative etching by Fe^{III} owing to the lower reduction potential of $PdCl_4^{2-}/Pd$ (0.59 V vs. SHE).[15] However, the difference (0.18 V) in the standard reduction potentials between Fe^{III}/Fe^{II} and $PdCl_4^{2-}/Pd$ pairs is too small to completely etch Pd nanocrystals with relatively large sizes. To enhance the driving force for the oxidative corrosion, apart from heating at 100 °C, a large amount of KBr was added into the etching system, as the standard reductant potential of $PdBr_4^{2-}/Pd$ pair is lower (0.49 V vs. SHE) than the chloride-based pair.[16] As a result, the Pd cubic cores could be completely removed through oxidative etching based on the following reaction:

$$Pd + 2\,Fe^{3+} + 4\,Br^- \xrightarrow{\Delta} PdBr_4^{2-} + 2\,Fe^{2+} \quad (1)$$

In summary, we have demonstrated the synthesis of Pd-Rh bimetallic nanocubes with a core–frame structure and concave faces by confined overgrowth of Rh atoms at the corners and edges of Pd cubic seeds. The site-specific overgrowth was achieved using a combination of kinetic manipulation of the formation rate of Rh atoms with a syringe pump and selective blocking of Pd {100} facets by Br^- ions. Structural and compositional analyses showed that the products were constructed from Pd cubic cores and Rh nanoframes with both Pd {100} and Rh {110} planes being exposed on the surface, suggesting great potential in catalytic applications. Subsequently, we used etching to selectively remove the Pd cores from the Pd-Rh core–frame concave nanocubes, generating cubic Rh nanoframes with a unique open structure. Two key factors are important for the selective etching: 1) the formation of a core–frame structure, in which the surface of Pd core is fully exposed; and 2) the difference in resistance to oxidative corrosion between Rh and Pd. We believe this strategy, based on site-specific overgrowth and selective etching, can be extended to other systems to generate nanocrystals with other novel structures and properties.

Received: July 27, 2012
Published online: September 11, 2012

Keywords: bimetallic nanocrystals · concave nanocubes · etching · palladium · rhodium

[1] a) P. D. Cozzoli, T. Pellegrino, L. Manna, *Chem. Soc. Rev.* **2006**, *35*, 1195; b) Y. Xia, Y. Xiong, B. Lim, S. E. Skrabalak, *Angew. Chem.* **2009**, *121*, 62; *Angew. Chem. Int. Ed.* **2009**, *48*, 60; c) Y. Sun, Y. Xia, *Science* **2002**, *298*, 2176; d) H. Lee, S. E. Habas, G. A. Somorjai, P. Yang, *J. Am. Chem. Soc.* **2008**, *130*, 5406; e) N. Tian, Z. Y. Zhou, S. G. Sun, Y. Ding, Z. L. Wang, *Science* **2007**, *316*, 732; f) E. C. Dreaden, M. A. Mackey, X. Huang, B. Kang, M. A. El-Sayed, *Chem. Soc. Rev.* **2011**, *40*, 3391.

[2] H. Zhang, M. Jin, Y. Xia, *Angew. Chem.* **2012**, *124*, 7774; *Angew. Chem. Int. Ed.* **2012**, *51*, 7656.

[3] a) M. Hu, J. Chen, Z. Y. Li, L. Au, G. V. Hartland, X. Li, M. Marquez, Y. Xia, *Chem. Soc. Rev.* **2006**, *35*, 1084; b) M. S. Yavuz, Y. Cheng, J. Chen, C. M. Cobley, Q. Zhang, M. Rycenga, J. Xie, C. Kim, K. H. Song, A. G. Schwartz, L. V. Wang, Y. Xia, *Nat. Mater.* **2009**, *8*, 935; c) Z. Peng, H. You, J. Wu, H. Yang, *Nano Lett.* **2010**, *10*, 1492.

[4] a) G. S. Métraux, Y. C. Cao, R. Jin, C. A. Mirkin, *Nano Lett.* **2003**, *3*, 519; b) X. Lu, L. Au, J. McLellan, Z. Y. Li, M. Marquez, Y. Xia, *Nano Lett.* **2007**, *7*, 1764; c) L. Au, Y. Chen, F. Zhou, P. H. C. Camargo, B. Lim, Z. Y. Li, D. S. Ginger, Y. Xia, *Nano Res.* **2008**, *1*, 441; d) M. McEachran, D. Keogh, B. Pietrobon, N. Cathcart, I. Gourevich, N. Coombs, V. Kitaev, *J. Am. Chem. Soc.* **2011**, *133*, 8066; e) N. Fan, Y. Yang, W. Wang, L. Zhang, W. Chen, C. Zou, S. Huang, *ACS Nano* **2012**, *6*, 4072.

[5] a) J. Zhang, M. R. Langille, M. L. Personick, K. Zhang, S. Li, C. A. Mirkin, *J. Am. Chem. Soc.* **2010**, *132*, 14012; b) X. Xia, J. Zeng, B. McDearmon, Y. Zheng, Q. Li, Y. Xia, *Angew. Chem.* **2011**, *123*, 12750; *Angew. Chem. Int. Ed.* **2011**, *50*, 12542; c) M. Jin, H. Zhang, Z. X. Xie, Y. Xia, *Angew. Chem.* **2011**, *123*, 7996; *Angew. Chem. Int. Ed.* **2011**, *50*, 7850; d) X. Huang, Z. Zhao, J. Fan, Y. Tan, N. Zheng, *J. Am. Chem. Soc.* **2011**, *133*, 4718; e) H. Zhang, W. Li, M. Jin, J. Zeng, T. Yu, D. Yang, Y. Xia, *Nano Lett.* **2011**, *11*, 898.

[6] a) C. J. DeSantis, A. A. Peverly, D. G. Peters, S. E. Skrabalak, *Nano Lett.* **2011**, *11*, 2164; b) D. Kim, Y. W. Lee, S. B. Lee, S. W. Han, *Angew. Chem.* **2012**, *124*, 163; *Angew. Chem. Int. Ed.* **2012**, *51*, 159; c) J. Li, Y. Zheng, J. Zeng, Y. Xia, *Chem. Eur. J.* **2012**, *18*, 8150.

[7] G. He, J. Zeng, M. Jin, H. Zhang, N. Lu, J. Wang, M. K. Kim, Y. Xia, *ChemCatChem* **2012**, DOI: 10.1002/cctc.201200205.

[8] a) B. Rodríguez-González, A. Burrows, M. Watanabe, C. J. Kiely, L. M. L. Marzán, *J. Mater. Chem.* **2005**, *15*, 1755; b) S. E. Habas, H. Lee, V. Radmilovic, G. A. Somorjai, P. Yang, *Nat. Mater.* **2007**, *6*, 692; c) F. R. Fan, D. Y. Liu, Y. F. Wu, S. Duan, Z. X. Xie, Z. Y. Jiang, Z. Q. Tian, *J. Am. Chem. Soc.* **2008**, *130*, 6949.

[9] J. Zeng, C. Zhu, J. Tao, M. Jin, H. Zhang, Z. Y. Li, Y. Zhu, Y. Xia, *Angew. Chem.* **2012**, *124*, 2404; *Angew. Chem. Int. Ed.* **2012**, *51*, 2354.

[10] a) J. Llopis, M. Vázquez, *Electrochim. Acta* **1964**, *9*, 1655; b) D. W. Rice, *J. Appl. Phys.* **1979**, *50*, 5899.
[11] M. Jin, H. Liu, H. Zhang, Z. X. Xie, J. Liu, Y. Xia, *Nano Res.* **2011**, *4*, 83.
[12] a) R. Narayanan, M. A. El-Sayed, *J. Am. Chem. Soc.* **2003**, *125*, 8340; b) F. Wang, C. Li, L. D. Sun, C. H. Xu, J. Wang, J. C. Yu, C. H. Yan, *Angew. Chem.* **2012**, *124*, 4956; *Angew. Chem. Int. Ed.* **2012**, *51*, 4872.
[13] a) M. E. Grass, Y. Zhang, D. R. Butcher, J. Y. Park, Y. Li, H. Bluhm, K. M. Bratlie, T. Zhang, G. A. Somorjai, *Angew. Chem.* **2008**, *120*, 9025; *Angew. Chem. Int. Ed.* **2008**, *47*, 8893; b) Y. Jang, S. Kim, S. W. Jun, B. H. Kim, S. Hwang, I. K. Song, B. M. Kim, T. Hyeon, *Chem. Commun.* **2011**, *47*, 3601.
[14] Y. Xia, E. Kim, G. M. Whitesides, *J. Electrochem. Soc.* **1996**, *143*, 1070.
[15] a) Y. Xiong, J. Chen, B. Wiley, Y. Xia, S. Aloni, Y. Yin, *J. Am. Chem. Soc.* **2005**, *127*, 7332; b) Y. Xiong, J. Chen, B. Wiley, Y. Xia, Y. Yin, Z. Y. Li, *Nano Lett.* **2005**, *5*, 1237.
[16] T. K. Sau, A. L. Rogach, *Complex-shaped Metal Nanoparticles*, Wiley-VCH, Weinheim, **2012**, p. 45.

